ELSEVIER

Polymer 41 (2000) 5461–5470

polymer

Hybrid films of poly(ethylene oxide-*b*-amide-6) containing sol–gel silicon or titanium oxide as inorganic fillers: effect of morphology and mechanical properties on gas permeability

R.A. Zoppi[a,*], S. das Neves[a,b], S.P. Nunes[c]

[a]*Instituto de Ciências Biológicas e Química, Pontifícia Universidade Católica de Campinas, Campus II, Av. John Boyd Dunlop, S/N, Campinas, São Paulo, SP, CEP 13020-904, Brazil*

[b]*Instituto de Química, Universidade de São Paulo, São Paulo, SP, Brazil*

[c]*GKSS-Forchungszentrum, 21502 Geesthacht, Germany*

Received 31 March 1999; received in revised form 1 September 1999; accepted 14 October 1999

Abstract

In this work we describe the preparation of hybrid organic–inorganic films using the sol–gel process. Poly(ethylene oxide-*b*-amide-6), PEBAX, was used as an organic matrix. Silicon oxide or titanium oxide were prepared by hydrolysis and polycondensation of tetraethoxysilane, TEOS, or titanium tetraisopropoxide, TiOP, respectively. Hybrid films were characterized by electron microscopy, stress–strain tests and their gas permeability and selectivity properties were evaluated. Small angle X-ray scattering was used to investigate structural heterogeneity caused by the presence of SiO_2 or TiO_2 particles in the organic matrix. For films containing silicon oxide as an inorganic filler, gas permeability decreased as a function of the inorganic component content. When titanium oxide was used as a filler, gas permeability was considerably lower than that measured for films containing silicon oxide (80/20 PEBAX/inorganic precursor compositions). In these cases, the morphologies were very similar, but films containing titanium oxide were much more rigid. For CO_2/N_2 and CO_2/H_2 separation factors up to 52.9 and 7.1, respectively, were obtained for 80/20 PEBAX/TiOP films. For higher titanium oxide contents, gas permeability increased. In these cases, a TiO_2 agglomeration was observed and the barrier performance decreased. Permeability and selectivity properties are discussed as a function of morphological and mechanical properties of these films.

Keywords: Sol–gel process; Hybrids; Membranes

1. Introduction

Membranes constituted only from organic polymers such as polysulfone, cellulose acetate, polyethersulfone, cellulose, polyamides, polyacrylonitrile, etc. and completely inorganic membranes constituted from alumina, borosilicate, and pyrolized carbon, are generally used in different membrane separation processes. Membranes can profit from advantages of both organic and inorganic segments. Organic components contribute to the formation of defect free inorganic membranes and make it less brittle. On the other side, organic membranes can have their chemical and temperature stability improved by an inorganic phase.

The incorporation of inorganic materials to improve mechanical properties and thermal stability of polymeric (organic) materials is a very common procedure. Silica, alumina and many other inorganic fillers have been added to a polymer matrix in large amounts to make it stiffer and in many cases also for economical reasons. Mechanical properties, however, are not always the main goal and the relatively large particles of these fillers may also interfere with other properties such as opacity, conductivity and permeability of different compounds across the final material.

In this context, the preparation of hybrid organic–inorganic materials using the sol–gel process has been a subject of growing interest. Using the sol–gel process it is possible to grow the inorganic phase into an organic polymeric matrix, with a very fine dispersion of the inorganic phase even at the molecular level.

The sol–gel process has been employed to prepare completely inorganic and also organic–inorganic hybrid membranes. In the first case, the preparation of membranes with a controlled porous size even in the nanometer range has been pointed as the major advantage of the sol–gel process. Membranes constituted by silica [1–4], alumina

* Corresponding author. Tel.: +55-19-729-8313; fax: +55-19-729-8517.
E-mail address: rita@iqm.unicamp.br (R.A. Zoppi).

0032-3861/00/$ - see front matter
PII: S0032-3861(99)00751-X

[5,6], zinc oxide [7], titanium oxide [8], and mixed oxides (TiO_2–ZrO_2) [9], have been prepared and characterized.

For hybrid membranes, the sol–gel process has been used in two different ways: (1) for preparing organic–inorganic membranes from polymers with Si–O and Si–C chemical bonds, and (2) for growing the inorganic phase into an organic polymer matrix. In the first case, different organic alkoxy silane precursors such as methyltriethoxysilane [10,11], diethoxydimethylsilane [12,13], 3-isocianopropyltriethoxysilane [14], phenyl alkoxy silanes [15], 3-aminopropylmethyldiethoxysilane [16,17], and 2-trimethoxysilylethyl-2-piridine and *N*-trimethoxysilylpropyl-*N*,*N*,*N*,-trimethylamonium chloride [18], were used with tetraethoxysilane to obtain silica based membranes. In the second case, the polymerization of the inorganic precursor occurs from a solution where the organic polymer is dissolved, or from a solution which can swell the organic matrix. The removal of the organic phase from an inorganic rich film may give rise to a fine microporous structure with high temperature stability. On the other hand, combining the permeability properties of the inorganic and organic phases may also be very advantageous. For instance, the introduction of a small amount of the inorganic phase may considerably inhibit an excessive swelling of the membrane by the permeants, increasing the selectivity. Examples of membranes which were prepared by this way are hybrids of NAFION® [19] or silicon rubber [20] and silica grown from TEOS, NAFION® and zirconium oxide grown from zirconium tetrabutyloxide [21].

In our groups, hybrid films have been formed from mixed organic polymer/TEOS solutions. Different organic matrices such as poly(ethylene oxide-*co*-epichlorhydrin) [22,23], NAFION® [24,25] and even poly(ethylene oxide-*b*-amide-6), PEBAX, have been used. PEBAX is an elastomer and its combination with sol–gel silica resulted in films with a large diversity of mechanical properties [26]. PEBAX is available with different degrees of hydrophilicity. Hydrophilic grades have been used for nano- and ultrafiltration membranes [27] as well as for gas separation [28].

Gas separation was investigated here with membranes prepared from hybrids of PEBAX/silicon oxide and also PEBAX/titanium oxide. As it will be described below, the permeability of the hybrids decreases when TEOS is added to the system. The introduction of TEOS followed by hydrolysis allows the formation of a very fine distributed inorganic phase. The mixture of both organic and inorganic phase in the molecular level decreases the permeability of the films (compared to the organic phase without inorganic components). If TiO_2 is the inorganic component, the opposite effect is observed. The permeability to different gases actually increases. The unfavorable contact between both phases probably leads to the formation of cavities at the interfaces and increases the gas permeation, decreasing the selectivity in some cases. Permeability and selectivity properties are discussed as a function of morphological and mechanical properties of these films.

2. Experimental part

2.1. Hybrid preparation

The copolymer with polyamide-6 and poly(ethylene oxide) blocks was kindly supplied by Elf Acquitaine with the trade name PEBAX® MX1657. The chemical composition of PEBAX was confirmed in a 2400 Perkin–Elmer CHN elemental analyzer. It contains 40 wt% polyamide-6 blocks and 60 wt% poly(ethylene oxide) blocks.

Since one of the copolymer block is a polyamide, it can dissolve only in very few solvents. Here the solvent was *n*-butanol.

Different volumes of tetraethoxysilane (Aldrich) were carefully added to a 3 wt% *n*-butanol/PEBAX solution under stirring at 60°C. Solutions with higher polymer contents, or with a polymer content up to 3 wt% at temperatures lower than 60°C, easily gel and could not be obtained with this solvent. A 0.15 mol/l HCl aqueous solution was added for keeping the 2:1 molar water/TEOS stoichiometric proportion. The solution (ca. 30 ml) was further stirred for 6.5 h at 60°C and transferred to a closed TEFLON® Petri dish with 10 cm diameter. The reaction was allowed to continue for 16 h. The dish was opened, the solvent was evaporated at 50°C and the films were further dried under vacuum during 1 week.

For PEBAX/titanium oxide films, the same procedure was used substituting TEOS by titanium tetraisopropoxide, TiOP, (Aldrich).

2.2. Stress–strain tests

Stress–strain measurements were performed using an Emic DL 2000 equipment with crosshead speed of 5 mm min^{-1} and a 50 N cell. Specimens with $7 \times 0.1 \times 50$ mm were used. The results presented in Table 2 are averages of more than ten measurements and they correspond to ($M \pm s$), where M is the arithmetic media and s the standard deviation estimative.

2.3. Scanning electron microscopy and field emission microscopy

Samples were fractured in liquid nitrogen and coated with gold by sputtering. Images were obtained in a JEOL T-300 scanning electron microscope. This microscope was equipped with an energy dispersive spectrometer (EDS) which allowed the chemical analysis of different regions in the sample.

Images were also obtained in a JEOL JSM-6340F field emission scanning electron microscope, which allows a better morphological resolution.

2.4. Wide angle X-ray diffraction

X-ray diffraction measurements were performed with a

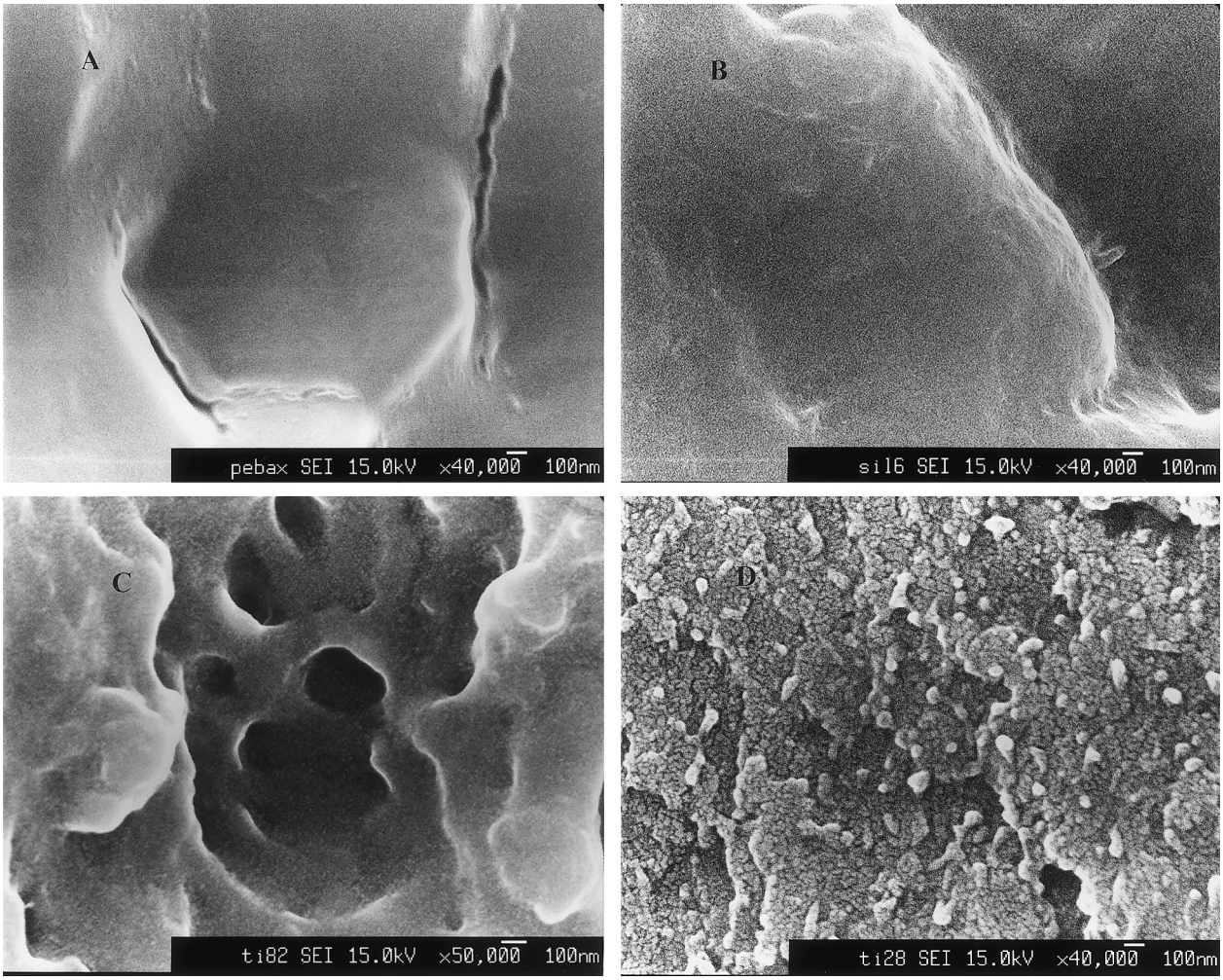

Fig. 1. Field emission microscopy of (A) pure PEBAX, (B) 20/80 PEBAX/TEOS, (C) 80/20 and (D) 20/80 PEBAX/TiOP films.

XD-3A Shimadzu X-ray diffractometer, using a CuK_{α} radiation.

2.5. Small angle X-ray scattering (SAXS)

SAXS measurements were carried out at LNLS–National Synchrotron Light Laboratory (Campinas, SP, Brazil), using synchrotron radiation facilities ($\lambda = 1.729$ Å).

The raw data were first corrected for decay of beam intensity and detector sensitivity by normalization with the incident X-ray intensity and the detector response function, respectively. To determine the fractal dimension and the radius of gyration, the scattering curves were fitted using Microcal Origin software (version 5.0).

2.6. Gas permeability measurements

Gas permeability kit used here was previously described in Ref. [35]. Gas permeability measurements were carried out with a commercially available test cell (Gelman Science Inc., Ann Arbor, MI), using single gases. The effective membrane area was 9.62 cm^2. The permeation rates were measured at 4 bar pressure difference with bubble flow meters. Before each measurement, the membrane was kept dry under vacuum. The results presented in Table 4 are averages of three measurements carried out in different specimens of each sample and they correspond to ($M \pm s$), where M is the arithmetic media and s the standard deviation estimative.

3. Results and discussion

3.1. Morphology

Fig. 1 shows the morphologies observed by field emission microscopy for pure PEBAX and hybrid films. For PEBAX/TEOS hybrids, independent on the composition range investigated here, domains were not detected by field emission or even transmission electron microscopy [26]. In these systems, the inorganic phase seems to be finely distributed in the organic matrix.

For PEBAX/TiOP hybrids, depending on the composition, phase separation was much more clear. The surface fracture of 80/20 PEBAX/TiOP films were not as smooth

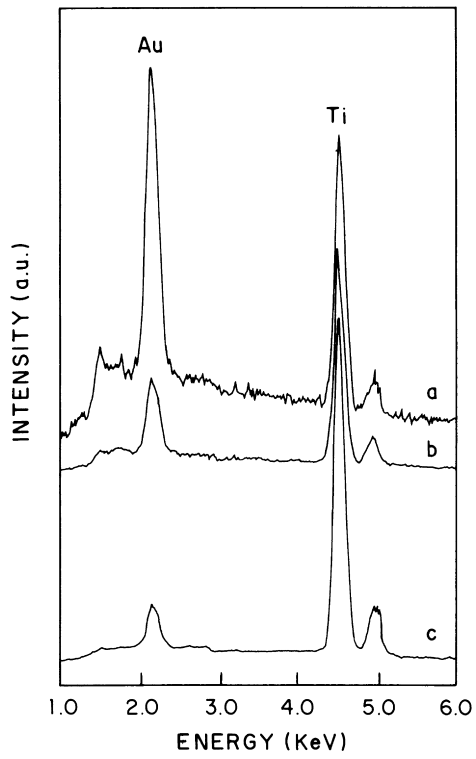

Fig. 2. EDS analysis for PEBAX/TiOP with different compositions: (a) 80/20, (b) 50/50 and (c) 20/80.

as that one observed for PEBAX/TEOS hybrids (comparing 80/20 PEBAX/TiOP with 20/80 PEBAX/TEOS, which even contains the highest inorganic alkoxide content), but a clear phase separation could not be detected. With the increase of the TiOP content, the surface fracture morphology gradually changes from this one showed in Fig. 1C to that in Fig. 1D. For 20/80 PEBAX/TiOP films, one could visualize particles, which have irregular form and size in the range from a few to 100 nm.

Hybrid films were also analyzed in a scanning electron microscope which was equipped with a energy dispersive spectrometer (EDS) to allow the chemical analysis in the sample. With EDS the presence of Si or Ti in hybrid films was confirmed, as shows Fig. 2 for PEBAX/TiOP. EDS was carried out in different regions of the sample. For both PEBAX/TEOS or PEBAX/TiOP hybrid systems a very homogeneous distribution of the inorganic phase was observed with no preferential accumulation of Si or Ti in any region across the films.

To have a relative information on how much of the inorganic precursor reacts to form the inorganic oxide, the intensity of the Ti and Si lines were compared with the intensity of the Au line. All samples were covered with Au by sputtering using the same conditions, so one can consider that the gold thickness is practically uniform in the hybrids surface fracture. Hybrids were also extensively dried before characterization and one could assume that the intensity of the Ti or Si lines are proportional to the content of inorganic oxide formed. Table 1 shows the theoretical inorganic oxide content, i.e. the inorganic oxide amount that would be formed if all inorganic alkoxide had been reacted. The Ti/Au and Si/Au intensity ratios for PEBAX/inorganic alkoxide of different compositions are also shown.

For PEBAX/TiOP films, the Ti/Au intensity ratio increases following practically the same proportion observed in the theoretical TiO_2 content increase. Although these results must not be used for an accurate quantitative analysis, they were in accordance to the theoretical inorganic oxide content. For PEBAX/TEOS systems, the increase on the Si/Au ratio did not follow the same tendency observed for PEBAX/TiOP systems anymore. These results are not so surprising, since we must consider the different rates of the hydrolysis and polycondensation reactions for TEOS and TiOP.

The sol–gel process follows a series of hydrolysis and condensation steps. Specially for silicon alkoxides, depending on the preparation conditions, different morphologies can be obtained. For instance, the presence of acids tends to produce more-linear or polymer-like molecules in the initial stages. These molecules can then coalesce in the drying process and eventually form a high-density material. In contrast, an alkaline environment tends to produce more of a dense-cluster growth leading to dense particulate-like structures. These particles can later bridge to form a very inhomogeneous system in terms of density fluctuations.

For PEBAX/TEOS and PEBAX/TiOP systems, recognition of the large differences in their hydrolysis and condensation rates is crucial. Here, titanium isopropoxide was made to react under the same conditions as for TEOS. Hydrolysis and condensation rapidly occurred leading to

Table 1
Comparison between the theoretical SiO_2 or TiO_2 contents in PEBAX/TEOS or PEBAX/TiOP hybrid films and EDS analysis

PEBAX/inorganic alkoxide	wt% of SiO_2[a]	wt% of TiO_2[a]	Ti/Au intensity ratio[b]	Si/Au intensity ratio[b]
80/20	7	7	0.8	0.40 ± 0.05
60/40	16	16	1.4	5.2 ± 0.4
50/50	22	22	2.3	7 ± 1
40/60	30	30	3.6	10.0 ± 0.6
20/80	54	53	5.9	9.8 ± 0.7

[a] The theoretical percentage was calculated considering a complete reaction of the inorganic alkoxide to form the inorganic oxide.
[b] The intensity ratio was calculated considering the element intensity line observed in EDS analysis.

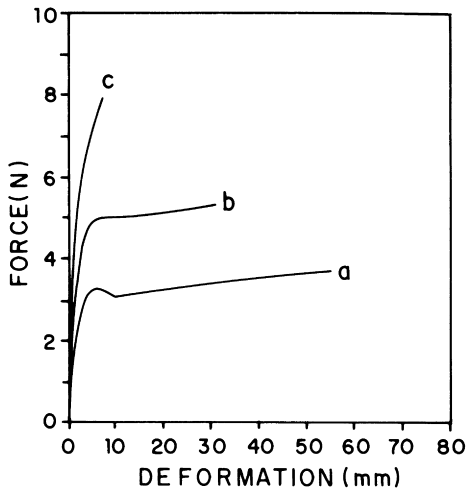

Fig. 3. Force as a function of deformation of (a) pure PEBAX, (b) 80/20 and (c) 60/40 PEBAX/TEOS films.

the formation of a TiO_2 particulate network. For TEOS, in slightly acid conditions, hydrolysis and condensation is much slower. The conversion of TiOP to TiO_2 may therefore be completed before the solvent evaporation and formation of the hybrid film. Phase separation occurs while the mobility is still quite high. In the case of TEOS due to the incomplete conversion probably a considerable amount of –OH groups are still available to favor the interaction with the polymer matrix. Results showed in Table 1 are in accordance to this proposition, since they evidence that TEOS was not converted to only SiO_2 anymore. Certainly hydrolysis and condensation byproducts are present. In addition, the presence of an inorganic phase containing silanol groups or even organic moieties would promote better PEBAX–inorganic phase interactions, leading to a much more homogeneous material, in accordance to electron microscopy characterization.

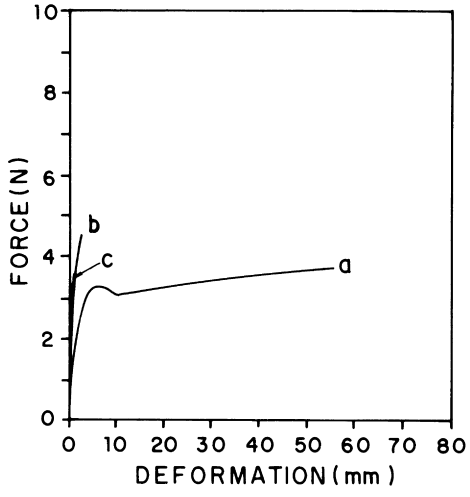

Fig. 4. Force as a function of deformation of (a) pure PEBAX, (b) 80/20 and (c) 60/40 PEBAX/TiOP films.

3.2. Mechanical properties

The mechanical properties of hybrid films were evaluated by stress–strain tests. Figs. 3 and 4 show force as a function of deformation for pure PEBAX and hybrid systems. Independently on the precursor, as expected, hybrids with higher than 20 wt% of inorganic precursor were much more rigid than pure PEBAX. Table 2 shows elasticity modulus, stress at break and strain at break for pure PEBAX and hybrid films. Films with inorganic precursor content higher than 50 wt% were extremely brittle to allow stress–strain tests or even gas permeability measurements.

Comparing hybrids with low inorganic content (around 20 wt%) those with TiOP were more rigid than those with TEOS. The morphology of both hybrids as observed by electron microscopy was quite similar. Also no considerable difference in crystallinity was observed. The differences in rigidity are due to intrinsic differences of both TiO_2 and SiO_2. There is also the possibility that TEOS has not been completely converted to SiO_2. As mentioned before, the conversion of TiOP to TiO_2 is much faster and may be completed before the solvent evaporates and decrease the mobility of the polymer matrix. If the formation of SiO_2 is not complete, a lower content of oxide is formed in the hybrid matrix leading to a lower rigidity.

3.3. Wide angle X-ray diffraction

Fig. 5 shows X-ray diffractograms for pure PEBAX and PEBAX/TiOP hybrids. PEBAX/TEOS systems were investigated in a previous work [26]. Table 3 shows the degree of crystallinity which was calculated from the ratio of the amorphous and crystalline areas of the diffractograms. For PEBAX/TiOP systems, degree of crystallinity was calculated taking into account that the crystallinity corresponds only to the organic polymer phase since here the incorporated inorganic phase is amorphous.

Considering the values for PEBAX/TiOP systems, it can be noted that the incorporation of the inorganic phase promoted a slight decrease of the degree of crystallinity, as verified for PEBAX/TEOS systems.

3.4. Small angle X-ray scattering

The SAXS data obtained for the two series of hybrid films are shown in Fig. 6. For each series, three regions can be recognized on scattering curves. At large q, the experiment is sensitive to the particle surfaces and gives information on the roughness of the beads (Porod region). In the intermediate regime, $I(q)$ is dependent on D_f, the fractal dimension of the network, while at very small q the material looks homogeneous (Guinier region) [29].

From the scattering curves, the influence of the TEOS or TiOP contents on the structure of the PEBAX matrix can be seen. An increase of the inorganic phase concentration leads to a change of the slope in the high q region of the scattering pattern, indicating the occurrence of alterations in the

Table 2
Elasticity modulus, stress at break and strain at break of PEBAX/TEOS or PEBAX/TiOP hybrid films

	Elasticity modulus (MPa)	Stress at break (MPa)	Strain at break (%)
PEBAX/TEOS			
100/0	190 ± 21	7.6 ± 0.6	150 ± 14
80/20	180 ± 17	8.2 ± 0.2	102 ± 15
60/40	300 ± 26	13 ± 2	16 ± 7
50/50	380 ± 66	8.9 ± 0.5	3.2 ± 0.5
PEBAX/TiOP			
80/20	270 ± 29	7.7 ± 0.8	10 ± 2
60/40	350 ± 46	9.2 ± 0.4	5.1 ± 0.5
50/50	320 ± 20	6 ± 1	2.1 ± 0.4

structure of the scattering particles. The scattering pattern observed for pure PEBAX samples corresponds to a quasi-ordered array of the crystalline regions of the organic polymer matrix. Due to the introduction and increase of concentration of an inorganic phase, a second correlation peak can be observed. It is more defined in PEBAX/TEOS hybrids. The origin of this second peak is due to the difference between the electron density of the inorganic phase and crystalline regions of the PEBAX matrix.

The radius of gyration (R_g) was determined from the point of crossover between the fractal behavior and the Guinier region. However, the spectrum is slightly concave at this point and the transitions therefore, are not sharp, which can be expected for a physical system consisting of a large number of scatters. Since in most of the cases the Guinier region is almost linear, the crossover point could be estimated using a linear fitting of this part of the curve. The R_g values are shown in Fig. 7.

However, it is difficult to determine the exact shape and nature of the structure of the scatter particles. R_g yields

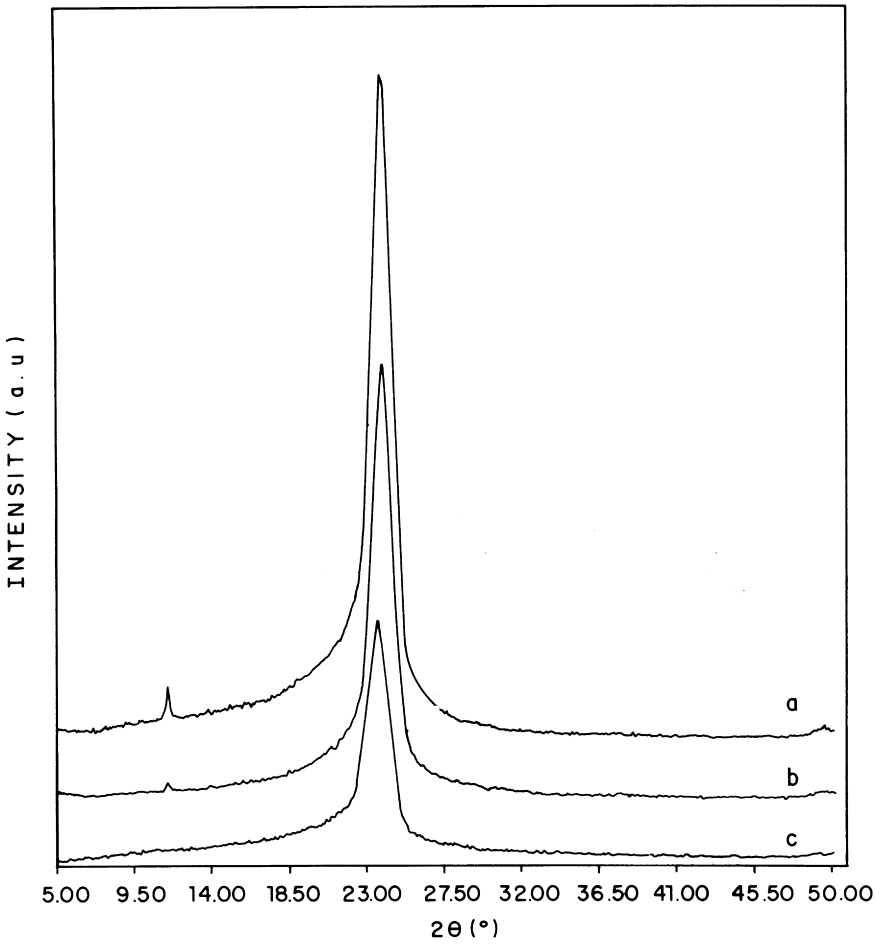

Fig. 5. X-ray diffractograms of (a) 80/20, (b) 60/40 and (c) 40/60 PEBAX/TiOP films.

Table 3
Degree of crystallinity (%) of PEBAX/TEOS or PEBAX/TiOP hybrid films

Composition	PEBAX/TEOS[a,b]	PEBAX/TiOP[b]	PEBAX/TiOP[c]
100/0	56	60	60
80/20	47	55	56
60/40	42	47	51
50/50	–	35	47
40/60	–	28	42

[a] Values obtained from Ref. [26].
[b] Degree of crystallinity calculated from the ratio between the amorphous and crystalline areas of the diffractograms, considering the hybrid as a whole.
[c] Degree of crystallinity, considering only the organic polymer phase.

information only about the size of the scattering fractals and the degree of overlap and interaction between the scatter structures. More information can be obtained by determining the fractality of these structures.

The fractal dimension of a particle can be determined from its scattering profile, analyzing the power-law regime. In this regime, the dependence of $I(q)$ on q follows [30–32]:

$$I(q) \propto q^{-\alpha} \quad (1)$$

where the exponent α is related to the fractal dimension of the scatter structures. For mass fractals, $\alpha = D_m$ (D_m being the fractal dimension for mass fractals) and $1 < \alpha < 3$ in a three-dimensional space. On the other hand, $\alpha = 6 - D_s$ (D_s being the fractal dimension for surface fractals) for surface fractals. If $D_s = 2$, the well-known Porod's law is obtained ($I(q) \propto q^{-4}$) for non-fractal structures with smooth interfaces.

Thus, by measuring the exponent α of the power-law regime, one can determine the nature of scattering. Depending on the value of the exponent α, it is possible to distinguish whether mass or surface fractals or just non-fractals are responsible for the scattering.

In Fig. 7, changes of the exponent α and R_g are plotted as a function of the inorganic precursor content. Variations on the α values indicate that the structure of the scattering particles changes from a surface fractal ($3 < \alpha < 4$) to a mass fractal ($2 < \alpha < 3$). The initial structure observed for the pure PEBAX matrix is surface fractal, which is characteristic of rough scattering structures (for instance crystallites distributed in an amorphous phase). With the addition of TEOS, the dominant scattering signal is characteristic of polymeric and non-compact mass fractals. For PEBAX/TiOP samples, the structures are surface fractals.

Comparing the SAXS results with electron microscopy characterization, one can associate the fractality of the samples with the phase separation. When the structures are mass fractals and therefore polymeric and non-compacts, the scatters are finely distributed in the PEBAX matrix and domains cannot be detected by microscopy characterization. For PEBAX/TiOP hybrids, the scatters are surface fractals corresponding to compact and rough structures which form domains visible in electronic microscopy.

From Fig. 7, changes on R_g can be observed. For PEBAX/TiOP, R_g decreases as a function of TiOP concentration, indicating a decrease of the scattering particles size with the increase of the inorganic phase content. At small TiOP contents, in acid hydrolysis conditions, larger polymer-like inorganic molecules can predominate. When the TiOP concentration increases, the inorganic phase can take the form of small particles. For PEBAX/TEOS hybrids, independent of the composition, R_g practically does not change indicating that the scatters have almost the same size. This is coherent with a non-occurrence of phase separation.

3.5. Gas permeability measurements

Tables 4 and 5 show permeability and selectivity values for different gases in PEBAX/TEOS or PEBAX/TiOP films.

In general, independently on the gas, for PEBAX/TEOS films the permeability decreased when the inorganic component content increased. In organic polymers filled with inert inorganic materials, gas permeability can increase or decrease depending on the polymer–filler adhesion and compatibility. An inert filler which has a good compatibility with the organic polymer matrix, usually decreases the permeability, mainly due to the reduction of the transport cross-section as well as the increase of the tortuous paths for gas molecules [33]. That was the case of PEBAX/TEOS films, which were shown to be homogeneous by electron microscopy and SAXS measurements. In addition, films containing higher amounts of TEOS, and consequently higher silica contents, were much more rigid, contributing to a gas permeability decrease.

Gas permeability of the PEBAX/TiOP films was lower than that of pure PEBAX, but it increased when the inorganic content increased from 20 to 50 wt%. The low gas permeability values obtained for 80/20 PEBAX/TiOP films could be assigned to their rigidity. These films were much more rigid than pure PEBAX (elasticity modulus was 190 for pure PEBAX and 270 MPa for 80/20 PEBAX/TiOP). The inorganic component decreased the permeability of the matrix as a whole, but for high inorganic contents the transport was probably favored in the area between the separated phases.

It is interesting to note that the elasticity modulus of films containing 50–60 wt% of TEOS or TiOP is practically the same, but the gas permeability of PEBAX/TiOP films was much higher than that of PEBAX/TEOS. This behavior could be associated to the morphological differences. For PEBAX/TiOP phase separation was very clear indicating a poor adhesion and compatibility between the organic polymer and the filler. In this case, there is a strong tendency to formation of cavities on the organic polymer–filler interface [33]. Furthermore, when the filler is not wholly wetted by the polymer, adsorption of diffusants can occur on its surface.

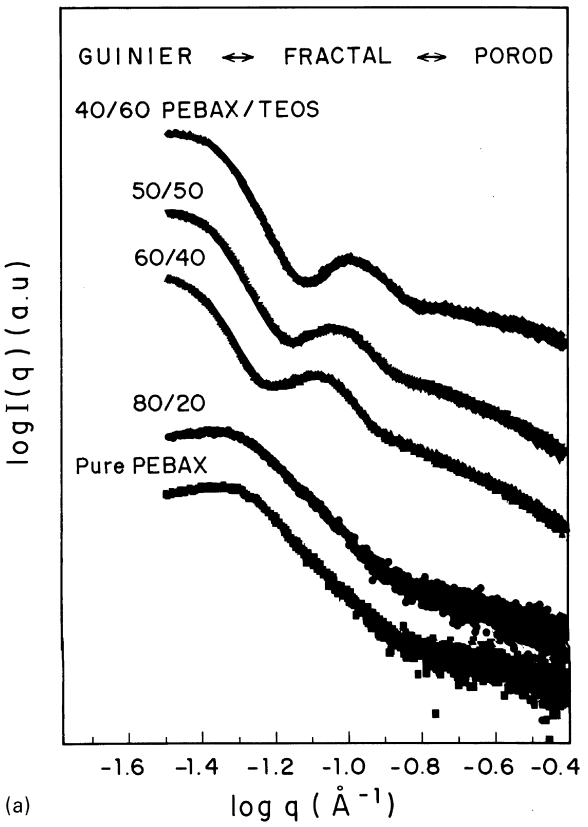

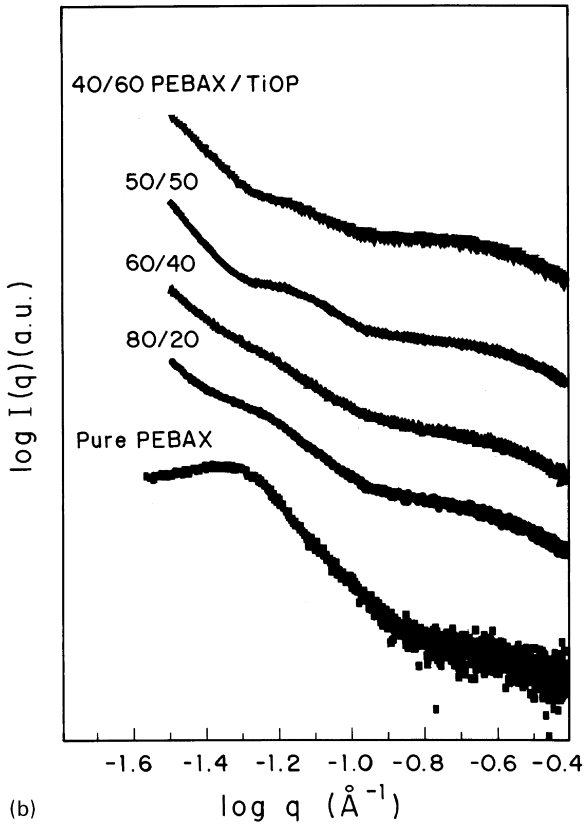

Fig. 6. Measured scattered intensities are plotted against wave vector of hybrid samples: (a) PEBAX/TEOS and (b) PEBAX/TiOP.

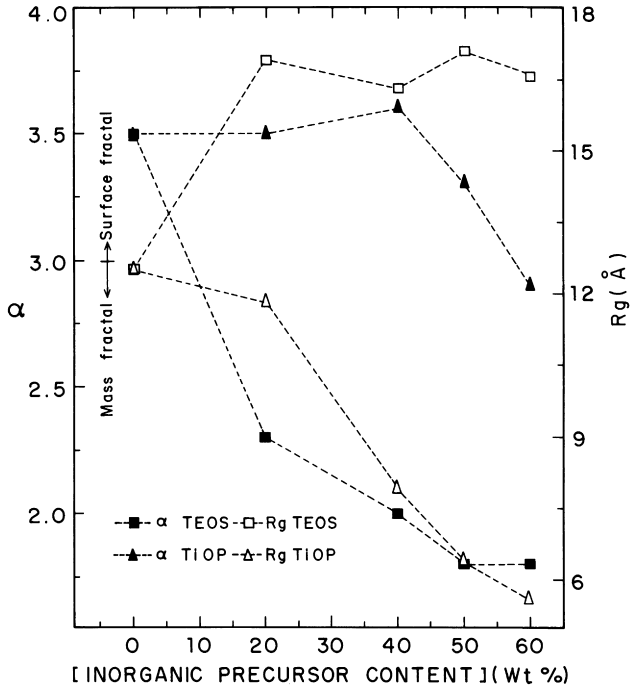

Fig. 7. Exponent α and radius of gyration (R_g) as a function of the inorganic precursor concentration.

For hybrid films, independently of using TEOS or TiOP, high permeability values for CO_2 were obtained. This behavior could be assigned to the presence of poly(ethylene oxide) segments in the organic matrix [34]. The transport of CO_2 is also influenced by the content of water dissolved in the PEBAX film. The CO_2/N_2 selectivity values measured here for pure PEBAX are lower than values reported by Pinnau and colleague [28] due to the extensive drying before characterization.

Oxygen–nitrogen separations represent a greatest challenge for membrane systems since the kinetic diameters of these gases differ by only a few tenths of one angstrom (3.46 for O_2 and 3.64 Å for N_2). The selectivity values for hybrid films (except for 80/20 PEBAX/TEOS) were similar to those obtained for hybrid membranes prepared from

Table 4
Gas permeability (P) of PEBAX/TEOS or PEBAX/TiOP hybrid films (1 Barrer = 10^{-10} cm^3 (cm s^{-1}) cm^{-2} cmHg^{-1})

	P (Barrer)				
	N_2	CH_4	O_2	H_2	CO_2
PEBAX/TEOS					
100/0	3.1 ± 0.4	7.2 ± 0.9	4.3 ± 0.9	13 ± 2	117 ± 15
80/20	2.7 ± 0.4	5.1 ± 0.9	2.9 ± 0.9	8 ± 1	51 ± 7
60/40	0.8 ± 0.2	2.0 ± 0.5	1.3 ± 0.4	3.7 ± 0.8	18 ± 3
50/50	0.4 ± 0.1	0.5 ± 0.1	2.0 ± 0.7	3.3 ± 0.5	20 ± 2
PEBAX/TiOP					
80/20	0.7 ± 0.2	2.2 ± 0.5	1.6 ± 0.3	5.2 ± 0.7	37 ± 7
60/40	0.9 ± 0.3	3.6 ± 0.6	3.1 ± 0.4	8 ± 1	44 ± 5
50/50	1.8 ± 0.3	6.4 ± 0.8	5 ± 1	12 ± 1	71 ± 6

Table 5
Selectivity (α) of PEBAX/TEOS or PEBAX/TiOP hybrid films

	α			
	O_2/N_2	CO_2/CH_4	CO_2/N_2	CO_2/H_2
PEBAX/TEOS				
100/0	1.4 ± 0.2	16.3 ± 0.2	37.7 ± 0.2	9.0 ± 0.2
80/20	1.1 ± 0.3	10.0 ± 0.2	18.9 ± 0.2	6.4 ± 0.2
60/40	1.6 ± 0.4	9.0 ± 0.3	22.5 ± 0.3	4.9 ± 0.3
50/50	5,0 ± 0.4	40.0 ± 0.2	50.0 ± 0.3	6.1 ± 0.2
PEBAX/TiOP				
80/20	2.3 ± 0.3	16.8 ± 0.3	52.9 ± 0.3	7.1 ± 0.2
60/40	3.4 ± 0.4	12.2 ± 0.2	48.9 ± 0.4	5.5 ± 0.2
50/50	2.8 ± 0.3	11.1 ± 0.2	39.4 ± 0.2	5.9 ± 0.1

hydrolysis and polycondensation of diamine/epoxy silanes [35]. Compared to dry NAFION® membranes (selectivity value for $O_2/N_2 = 4.15$) [36], 50/50 PEBAX/TEOS films were also slightly more selective.

Carbon dioxide–methane separation is an area where specialty polymers have been successfully developed. For 50/50 PEBAX/TEOS films, the CO_2/CH_4 separation factor was considerably higher than for the other hybrids. It is still lower than those obtained for membranes based on polyimides or poly(methyl methacrylate) [37,38], where the α CO_2/CH_4 values are 60 and 130, which have CO_2 permeabilities of about 23 and 0.7 Barrer, respectively.

The selectivity of PEBAX/TiOP to CO_2/N_2 was higher than that of pure PEBAX, which is already considered high. Selectivity values of some other polymers to CO_2/N_2 are listed here: ethyl cellulose (4.9), poly(dimethylsiloxane) (11.5), poly(terc-butyl acetylene) (13.6), polybutadiene (21.5), poly(phenylene oxide) (19.9), poly(methyl pentene) (11.8) and neoprene (21.5), as reported in Ref. [35].

4. Conclusions

PEBAX/TEOS and PEBAX/TiOP hybrids were prepared by hydrolysis and condensation of the inorganic precursors from solutions containing the organic polymeric matrix. Both PEBAX/TEOS and PEBAX/TiOP systems had their elasticity modulus increased when the inorganic component content increased. Comparing hybrids with 20 wt% inorganic precursor, those with TiOP were more rigid than with TEOS. The degree of crystallinity of the polymeric matrix slightly decreased with the incorporation of an amorphous inorganic phase.

The different rates of hydrolysis and condensation reactions for TEOS and TiOP gave rise to different morphologies, mainly with higher inorganic precursor contents. When TiOP was used, a clear phase separation was observed. For TEOS, however, very homogeneous films were obtained even for inorganic contents as high as 80 wt%. In accordance to electron microscopy, SAXS measurements confirmed that PEBAX/TEOS hybrids are homogeneous. In these cases, independent on the inorganic precursor content, the scattering structures are mass fractals with non-significant variation of the radius of gyration. PEBAX/TiOP are heterogeneous with scattering patterns characteristic of surface fractals.

The introduction of the inorganic phase had clear effect on the gas permeability. For hybrids with TEOS, which was homogeneously distributed even at high inorganic contents, the gas permeability decreased continuously. For hybrids with TiOP, the permeability initially decreased, but increased with introduction of more inorganic precursor. Since phase separation takes place with TiOP, the inorganic content in the polymer matrix to be permeated did not increase continuously with increasing amount of TiOP. The inorganic component partially separates in domains. The permeability of molecules such as nitrogen, which are more diffusion controlled seems to decrease more than the CO_2 permeability, which depends more on its solubility in the polymer matrix. Therefore a significant increase of selectivity (37.7–52.9) for CO_2/N_2 was observed with addition of 20 wt% of TiOP. At higher TiOP contents, as phase separation is favored, the selectivity decreased almost down to values of pure PEBAX.

Acknowledgements

The authors thank FAPESP for financial support (Proc. 95/9506-4, 96/6942-0, 95/3636-3 and 97/03395-1). We thank Prof Iris Torriani from IFGW-UNICAMP for valuable discussions related with SAXS experiments. Research partially performed at LNLS–National Synchrotron Light Laboratory, Brazil.

References

[1] Elferink WJ, Nair BN, De Vos RM, Keizer K, Verweij H. J Colloid Interf Sci 1996;180:127.
[2] Nair BN, Elferink WJ, Keizer K, Verweij H. J Colloid Interf Sci 1996;178:565.
[3] Hyun SH, Kang BS. J Am Ceram Soc 1994;77:3093.
[4] Ayral A, Balzer C, Dabadie T, Guizard C, Julbe A. Catal Today 1995;25:219.
[5] Yu CC, Klein LC. J Am Ceram Soc 1995;78:3149.
[6] Yu C, Klein LC. J Am Ceram Soc 1992;75:2613.
[7] Sakohara S, Tickanen LD, Anderson MA. J Phys Chem 1992;96:11 086.
[8] Hyun SH, Kang BS. J Am Ceram Soc 1996;79:279.
[9] Xu Q, Anderson MA. J Am Ceram Soc 1993;76:2093.
[10] Dirè S, Pagani E, Babonneau F, Ceccato R, Carturan G. J Mater Chem 1997;7:67.
[11] Dirè S, Pagani E, Ceccato R, Carturan G. J Mater Chem 1997;7:919.
[12] Kimura K, Sunagawa T, Yokoyama M. Chem Lett 1995:967.
[13] Kimura K, Sunagawa T, Yokoyama M. Anal Chem 1997;69:2379.
[14] Kim W, Sung DD, Park SB. The Analyst 1998;123:379.
[15] Smaihi M, Jermoumi T, Marignan J, Noble RD. J Membr Sci 1996;116:211.
[16] Guizard C, Lacan P. New J Chem 1994;18:1097.
[17] Lacan P, Guizard C, Le Gall P, Wettling D, Cot L. J Membr Sci 1995;100:99.

[18] Kogure M, Ohya H, Paterson R, Hosaka M, Kim J-J, McFadzean S. J Membr Sci 1997;126:161.
[19] Gummaraju RV, Moore RB, Mauritz KA. J Polym Sci, Part B 1996;34:2383.
[20] Nunes SP, Schultz J, Peinemann K-V. J Mater Sci Lett 1996;15:1139.
[21] Apichatachutapan W, Moore RB, Mauritz KA. J Appl Polym Sci 1996;62:417.
[22] Zoppi RA, Nunes SP. Polymer 1998;39:6195.
[23] Zoppi RA, Fonseca CNMP, De Paoli M-A, Nunes SP. Acta Polym 1997;48:131.
[24] Zoppi RA, Yoshida IVP, Nunes SP. Polymer 1997;39:1309.
[25] Zoppi RA, Nunes SP. J Electroanal Chem 1998;445:39.
[26] Zoppi RA, de Castro CR, Yoshida IVP, Nunes SP. Polymer 1997;38:5705.
[27] Nunes SP, Sforça ML, Peinemann KV. J Membr Sci 1995;106:49.
[28] Blume I, Pinnau I. US Patent 4,963,165, Composite membrane, method of preparation and use, 16 October 1990, assigned to Membrane Technology & Research.
[29] Zarzycki J. J Non-Cryst Solids 1990;121:110.
[30] Schaefer DW, Keefer KD. Phys Rev Lett 1984;53:1383.
[31] Schaefer DW. Science 1989;243:1023.
[32] Schmidt PW. J Appl Crystallogr 1991;24:414.
[33] Naylor TV. In: Allen G, Bevington JC, Booth C, Price C, editors. 1. Comprehensive polymer science, the synthesis, characterization, reactions & applications of polymers, 2. Oxford: Pergamon Press, 1989. p. 643.
[34] Okamoto K, Fujii M, Okamyo S, Suzuki H, Tanaka K, Kita H. Macromolecules 1995;28:6950.
[35] Sforça ML, Yoshida IV, Nunes SP. J Membr Sci 1999;159:197.
[36] Chiou JS, Paul DR. Ind Eng Chem Res 1988;27:2161.
[37] Robeson LM. J Membr Sci 1991;62:165.
[38] Stern SA. J Membr Sci 1994;94:1.